

## Design and Measurements of Rectangular Dielectric Resonator Antenna Linear Arrays

Feras Z. Abushakra<sup>1</sup>, Asem S. Al-Zoubi<sup>1</sup>, and Derar F. Hawatmeh<sup>2</sup>

<sup>1</sup>Department of Telecommunications Engineering  
Yarmouk University, Irbid, Jordan  
feras\_abushakra@yahoo.com, asem@yu.edu.jo

<sup>2</sup>Department of Electrical Engineering  
University of South Florida, Tampa, FL, USA  
dfh\_ee@hotmail.com

**Abstract** — In this paper, two, four, eight and sixteen-element Rectangular Dielectric Resonator Antenna (RDRA) linear arrays fed by microstrip line have been designed and simulated. The DRA is excited by a vertical strip placed on the middle of the DRA wide side wall through a coaxial probe attached to the microstrip line on the other side of the substrate. The ground plane is sitting directly underneath the RDRA while the microstrip line feeder is at the opposite side of the substrate to avoid the unwanted radiation from the feeder. The simulated and measured 10 dB return loss bandwidth of the antenna arrays are 67.8%, 75%, 73.5%, and 76% for the two, four, eight and sixteen-element arrays respectively. The simulated gain of the single element antenna is about 6 dBi, while it reaches to about 17 dBi for the 16-element array.

**Index Terms** — Avoidance of spurious radiation dielectric resonator antennas, linear array, low cross polarization level, low side lobe level.

### I. INTRODUCTION

Dielectric resonator antenna (DRA) is fabricated from a high-relative permittivity (from about 6 to 100) low loss dielectric material [1]. The dielectric resonator antennas DRAs have several advantages which make them a good choice for the new wireless communication systems, especially if small size antenna is required. There are some features of the DRA that give it an advantage compared to the microstrip antennas such as wider impedance bandwidth, high gain, avoidance of surface waves and high radiation efficiency [2]. In new wireless communication systems the high gain and wide bandwidth are essential demands. Sometimes, it is difficult to obtain the desired gain value for certain application when single element is used. Arrays with different number of elements could be used to achieve the wanted radiation parameter for the new communication

systems. The most common type of arrays is the linear array. The linear array is set with different number of elements with fixed spacing between them. The elements are positioned in a straight line along one of the axes [3]. It has several properties that make it a good choice for many applications, such as, narrow main beam. The main beam becomes narrower as the number of elements in the array increases [4]. Recently, many researches focused on the design of DRA arrays. This is because they could offer high gain value which is hard to achieve when using other types of antennas. In [5], a dual segment two-element cylindrical DRA array was designed. This array covered a frequency band of (3.85-6.2) GHz and the gain varied between (4-6) dBi. In [6], two-element RDRA linear array was designed. The proposed array covered the frequency band from (3.15-3.83) GHz, with gain value of 6.4 dBi. In [7], a linear array of RDRA with dielectric image guide (DIG) feeder was designed. By adding a narrow metal strip around the DRA, the cross polarization level decreased by 20 dB. In [8], a back reflector was used with a linear array with (DIG) feeder; a reflecting PEC was inserted above the (DIG) to decrease the back lobe radiation. Four-element RDRA with high relative permittivity of ( $\epsilon_r=35.9$ ) was designed in [9]. The RDRA has dimensions of (18×18×8.9) mm. The elements were fed by aperture of window shape, the designed array covered frequency band from (1.5-3.2) GHz, the gain reached to 14 dBi. However, the distance between the adjacent elements was (66.6) mm. In [10], a linear DRA polarized array fed by radial line waveguide was designed. This array had 180 elements with 223 mm diameter. The gain reached 26.7 dBi. In [11], a series DRA array was designed. The array was fed by substrate integrated waveguide (SIW). The 4×1 array achieved 11.7 dBi gain, with 4.7% impedance bandwidth. In [12], eight-element RDRA series fed array reached more than 14 dBi gain value. A slot windows and reflector were used to improve the performance for this array. In this

paper up to sixteen elements RDRA linear arrays will be designed, simulated and measured. A microstrip line feeder with multi-section will be used to feed the RDRA's and to enhance the bandwidth [13]. The feeder will be at the bottom side of the substrate while the ground plane is at the top side of the substrate. A coaxial probe is attached between the microstrip line and a center strip mounted on the side of the DRA. By using this feeding method the spurious radiation from the feeder will be isolated.

**II. SINGLE ELEMENT RDRA**

Several methods for the mathematical calculation of the resonant frequency of the RDRA have been reported. These methods include the dielectric waveguide model (DWM) [14] and applying the perturbation theory to the (DWM) to determine the accurate resonant frequency of the RDRA [15]. However, the focus in this paper will be on the design of the arrays with wide band by simulation and measurement. Figure 1 presents the single element RDRA geometry. The RDRA material is Rogers RO 3010 with relative permittivity of ( $\epsilon_r=10.2$ ) and dielectric loss tangent of ( $\tan\delta=0.0035$ ). The dimensions of the RDRA are ( $a \times b \times d$ ) which corresponds to ( $15.7 \times 14.3 \times 11$ ) mm, respectively. The substrate is Rogers RO 4350 with relative permittivity of ( $\epsilon_r=3.66$ ) and dielectric loss tangent of ( $\tan\delta=0.004$ ), the dimensions of the substrate are ( $50 \times 40 \times 1.524$ ) mm. The materials of the RDRA and substrate for the single RDRA element will be used in all designs in this paper.

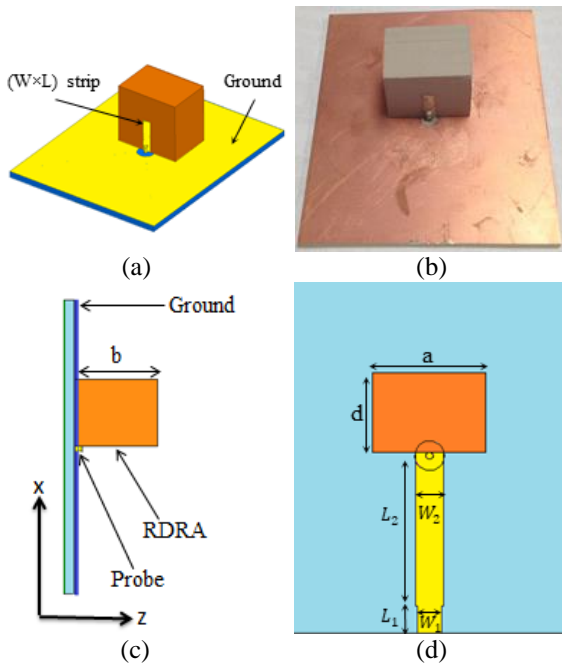


Fig. 1. Geometry of the single RDRA: (a) 3D view, (b) fabrication, (c) side view, and (d) top view.

In the single element RDRA design the ground plane is at the top side of the substrate. The microstrip line feeder is at the bottom side of the substrate as shown in Fig. 1. By sitting the RDRA directly on the ground plane the spurious radiation from the feeder will be isolated and the cross polarization level will be reduced [16-18]. A probe is attached to microstrip line and pass through a circular aperture that is created in the ground plane with 2.05 mm radius. The probe then is attached to a rectangular strip mounted on the DRA side surface with ( $W \times L$ ) dimensions. The dimensions of single element RDRA are mentioned in Table 1.

Table 1: Dimensions of the single RDRA in (mm)

Parameter	Value	Parameter	Value
L	7.76	W	2
L <sub>1</sub>	3.72	W <sub>1</sub>	3.36
L <sub>2</sub>	21.27	W <sub>2</sub>	3.84

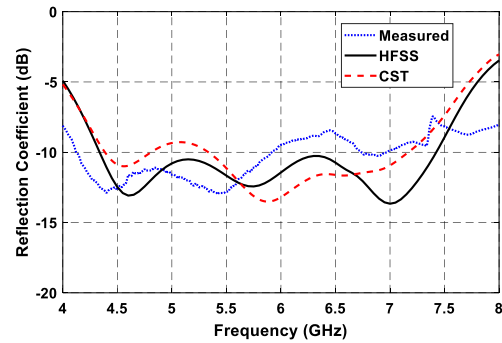


Fig. 2. The reflection coefficient for the single RDRA.

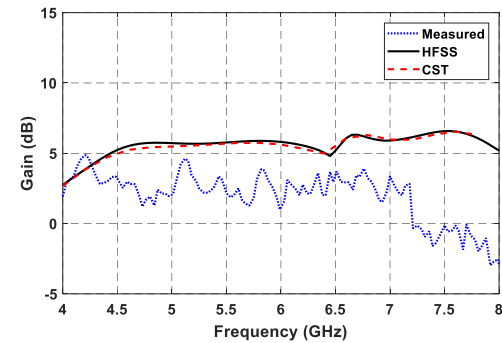


Fig. 3. The peak gain for the single RDRA.

The simulation results of both software, HFSS [19] and CST MWS [20], are in good agreement. The HFSS works based on the finite element method (FEM) while the CST uses the finite integration technique (FIT) which is relevant to finite domain time difference (FDTD) [21]. The -10 dB reflection coefficient for the single RDRA is achieved in a frequency band of 4.3-7.4 GHz (53%), as shown in Fig. 2. The simulated peak realized gain for the

single RDRA is between (5-6.5) dBi, as shown in Fig. 3. The difference between the measured and the simulated results is due to the fabrication tolerances, gluing in the RDRA's since we used four layers of substrate materials to fabricate each RDRA, surface roughness of the ground plane and the effect of the connector. However, the results still close to each other.

### III. MUTUAL COUPLING

Mutual coupling is described as the amount of energy that absorbed by the neighbor element. It is an important parameter when array design is considered. The higher mutual coupling level will decrease the gain of the array and decrease the radiation efficiency for the main beam [22]. The distance between center to center of two elements should be theoretically between  $\lambda/2$  and  $\lambda$ . The chosen distance will be within the theoretical range. However, the exact value for the distance which is 23.8 mm is chosen based on a parametric study to reach the best matching and radiation pattern for the designs. This distance represent  $0.76 \lambda$  at  $f=5$  GHz. In Fig. 4, two elements RDRA are placed beside each other to determine the mutual coupling between them.

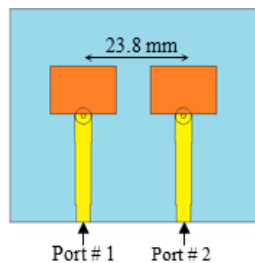


Fig. 4. Geometry of two single RDRA.

The parameter  $|S_{21}|$ , which represents the mutual coupling between the two RDRA is plotted in Fig. 5, which indicates that the mutual coupling is less than -13 dB in the operating band which considered low value for the mutual coupling.

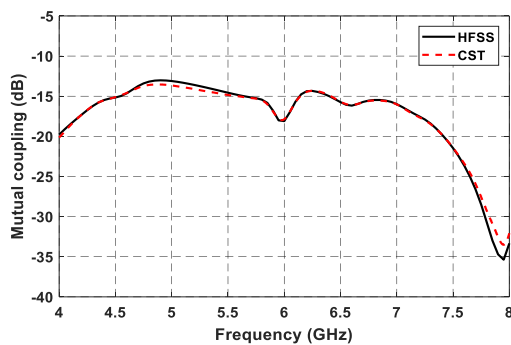


Fig. 5. The simulated mutual coupling.

### IV. TWO-ELEMENT RDRA

Two-element RDRA linear array is designed and simulated. Figure 6 shows the geometry of the two-element linear array. Same feeding method and materials for the single RDRA is used here. The feeder is at the bottom side of the substrate. The dimensions of the two-element linear array are shown in Fig. 6 (b) and mentioned in Table 2. The same RDRA dimensions and slot aperture radius in the single element will be used here. The rectangular strip dimensions are adjusted to (3×7.5) mm. These dimensions will be used in all arrays in this paper.

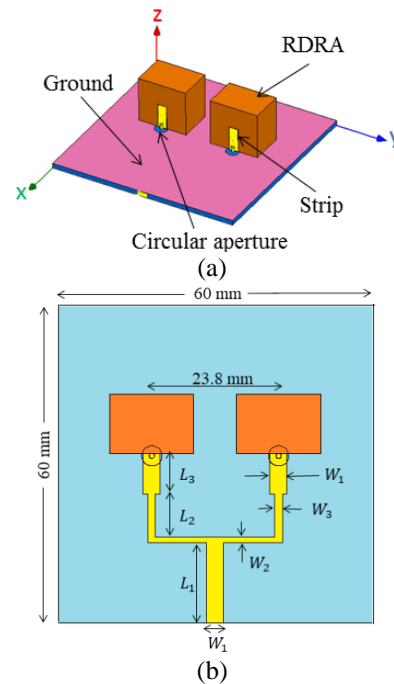


Fig. 6. (a) Geometry of two-element RDRA linear array, and (b) two-element DRA feeder.

Table 2: Dimensions of the two-element RDRA linear array in (mm)

Parameter	Value	Parameter	Value
$L_1$	15	$W_1$	3.2
$L_2$	8	$W_2$	1.2
$L_3$	7.7	$W_3$	1.4

Figure 7 shows the simulated reflection coefficient for the two-element RDRA linear array. The -10 dB reflection coefficient is achieved in the frequency range 3.9-7.9 GHz (67.8%). The simulated peak realized gain for the two-element RDRA linear array varying between (6.5-10) dBi, as shown in Fig. 8. The gain increases at the end of the band, which is expected since the distance between the elements exceeds  $\lambda$ .

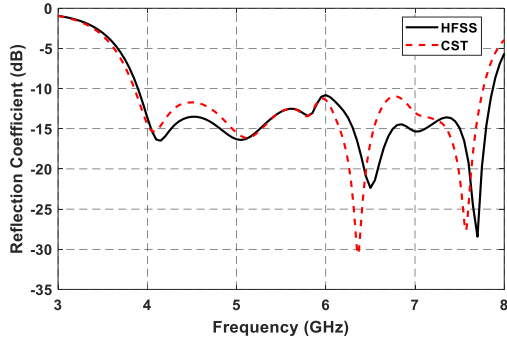


Fig. 7. The simulated reflection coefficient for the two-element linear array.

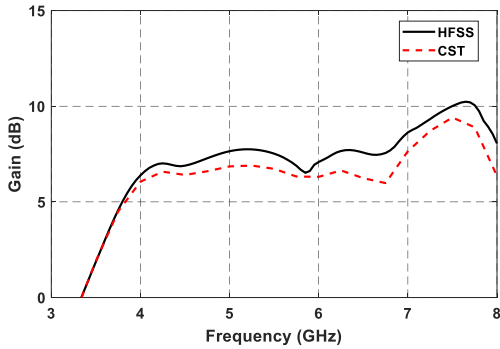


Fig. 8. The simulated peak gain for the two-element linear array.

**V. FOUR-ELEMENT RDRA**

The Geometry for the four-element RDRA linear array is shown in Fig. 9. The dimensions are mentioned in Table 3. It could be seen that the array substrate has dimensions of (70×100) mm only, which is considered small array size for this number of elements. The dimensions which were mentioned in the two-element array are used here. So, it will not be repeated. Also, same direction for the feeder as in Fig. 6 (a) will be used here.

The simulated reflection coefficient for the four-element RDRA linear array is shown in Fig. 10. The operating frequency is from 3.57-7.85 GHz (75%). The simulated peak gain has a stable value between (8-10) dBi within the operating band and reaches 12 dBi at  $f=7.7$  GHz as shown in Fig. 11. A good agreement between both software is achieved in the simulated results.

Table 3: Dimensions of the four-element RDRA linear array in (mm)

Parameter	Value	Parameter	Value
$L_4$	14	$W_1$	3.2
$L_5$	46.4	$W_4$	1
$L_6$	4.5	$W_5$	1.2

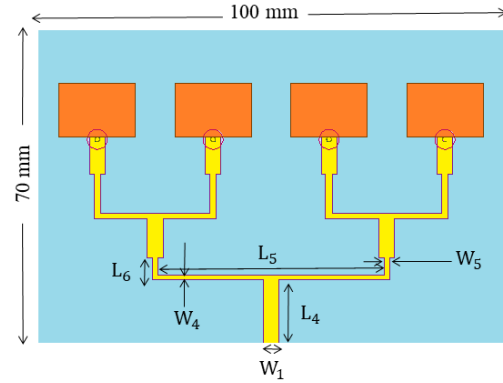


Fig. 9. Geometry of four-element RDRA linear array.

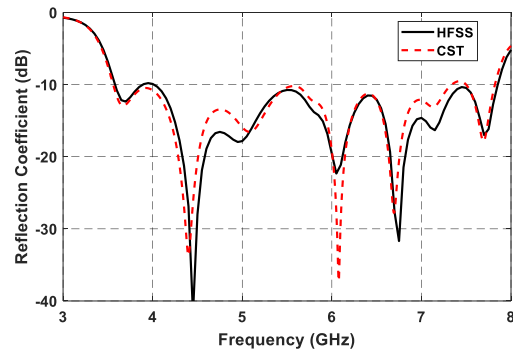


Fig. 10. The simulated reflection coefficient for the four-element linear array.

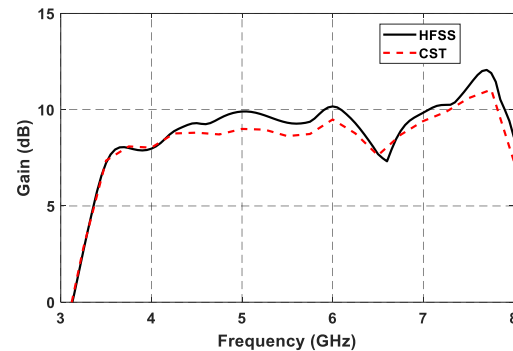


Fig. 11. The simulated peak gain for the four-element linear array.

**VI. EIGHT-ELEMENT RDRA**

The eight-element linear array is designed, simulated and fabricated, as shown in Fig. 12. In Fig. 12 (a) the fabricated array from the top view is presented. As mentioned in the previous arrays, the DRAs are sitting directly on the ground plane. The feeder is at the back side as shown in Fig. 12 (b). The dimensions for this array are plotted in Fig. 12 (c) and mentioned at Table 4 in (mm).

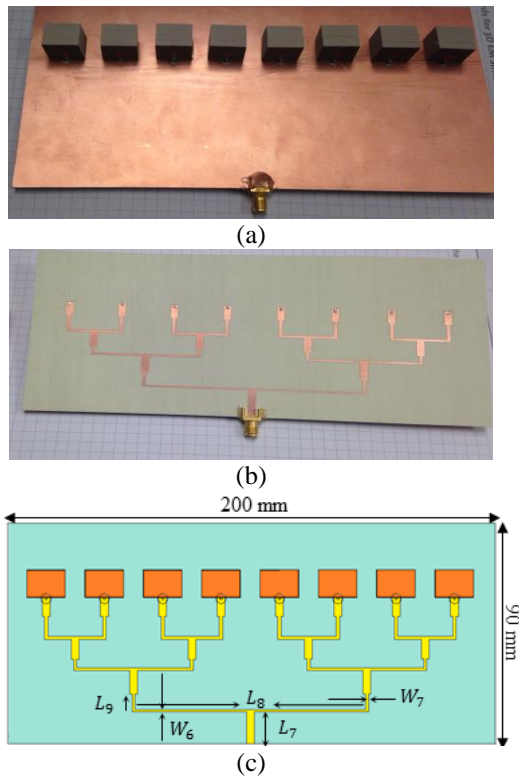


Fig. 12. Eight-element array: (a) fabricated 3D view, (b) fabricated bottom view, and (c) feeder dimensions.

Table 4: Dimensions of the eight-element RDRA linear array in (mm)

Parameter	Value	Parameter	Value
$L_7$	14.5	$W_6$	0.8
$L_8$	93.95	$W_7$	1.25
$L_9$	7.2	----	----

The measured and simulated reflection coefficients for the eight-element RDRA linear array are plotted in Fig. 13. A good agreement between HFSS, CST MWS and the measured results could be noticed in this figure. The -10 dB reflection coefficient is achieved in the frequency range (3.7-8) GHz, which is equivalent to 73.5% impedance bandwidth for the simulated results while the measured result shows a little difference compared to the simulated results only at the beginning of the band. However, the results still close to each other.

Figure 14 shows the measured and simulated peak realized gain. The gain has stable value which is above 12 dBi through most of the band according to both HFSS and CST MWS, while it reaches 14 dBi at the end of the band. A good agreement is noticed between simulated and measured gain values for this array, except at the end of the band where the difference between the simulated and measured results is noticed, which is due to the previously mentioned reasons in Section II in the fabrication process of the RDRA.

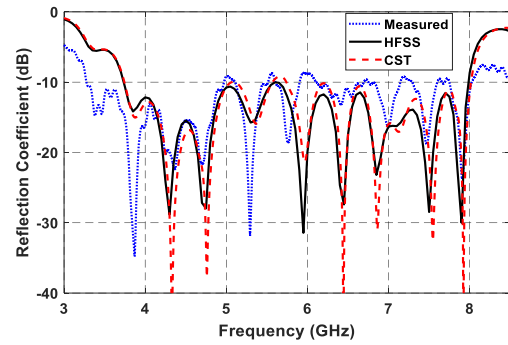


Fig. 13. The reflection coefficient for the eight-element linear array.

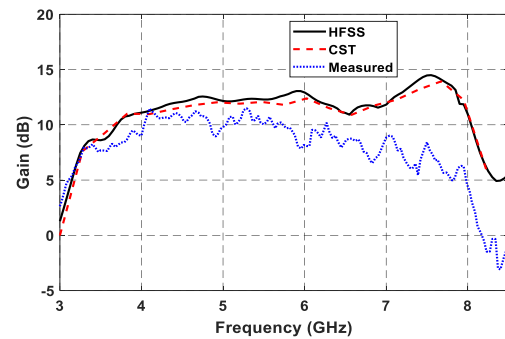


Fig. 14. The peak gain for the eight-element linear array.

**Simulated and measured radiation patterns**

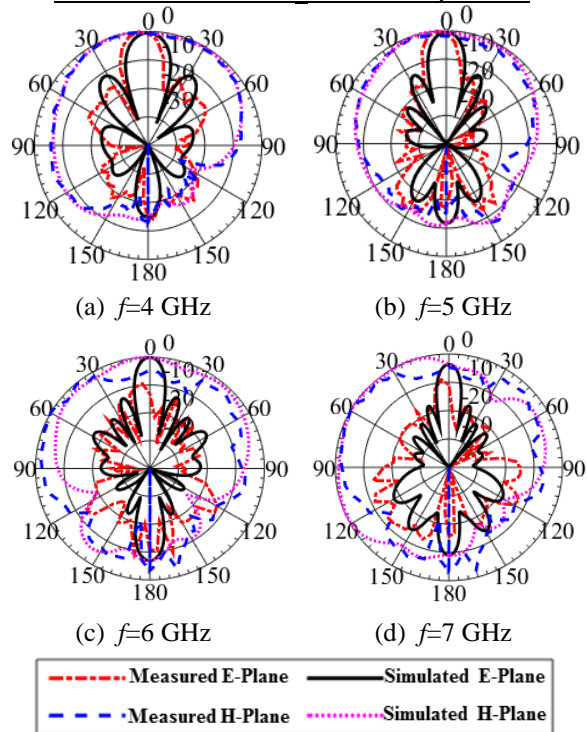


Fig. 15. The normalized radiation patterns of the eight-element linear array at different frequencies.

The measured and simulated radiation patterns are plotted in Fig. 15. The co-polarized E-Plane and H-Plane are plotted. The radiation patterns show a 10-dB front to back ratio through the band. The side lobe level (SLL) is around (-15) dB in the band. The simulated and measured cross polarization level was found less than -10 dB within the band. The simulated results for the radiation pattern will be presented using one software only which is HFSS, since both software give the same results and this would be easier to read.

**VII. SIXTEEN-ELEMENT RDRA**

Finally, sixteen-element RDRA linear array is simulated. The substrate size for this design is (390×110) mm, as shown in Fig. 16. The dimensions are mentioned in Table 5.

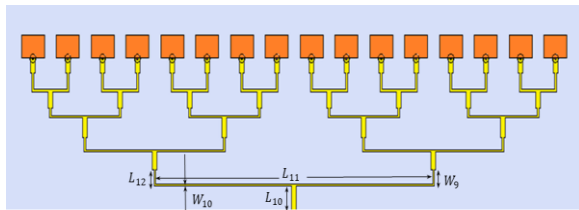


Fig. 16. Geometry of the sixteen-element linear array.

Table 5: Dimensions of the sixteen-element RDRA linear array in (mm)

Parameter	Value	Parameter	Value
$L_{10}$	12.9	$W_8$	0.62
$L_{11}$	189.3	$W_9$	1
$L_{12}$	6.4	-----	-----

The operating frequency range is from (3.57-7.95) GHz, as shown in Fig. 17, which is about 76% impedance bandwidth. The simulated peak realized gain for the sixteen-element linear array is stable between 14-17 dBi as shown in Fig. 18. It could be seen that the theoretical 3 dBi gain increment when doubling the elements number in the linear arrays didn't achieved, since the presences of the losses in the substrate, feeder and the RDRA itself [23].

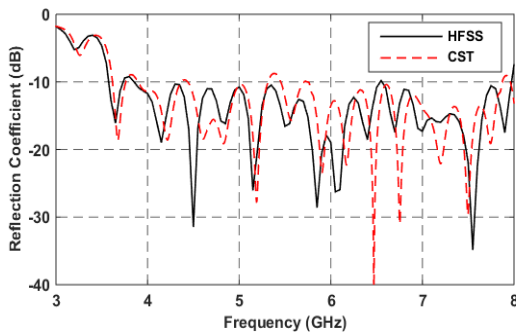


Fig. 17. The simulated reflection coefficient for the sixteen-element linear array.

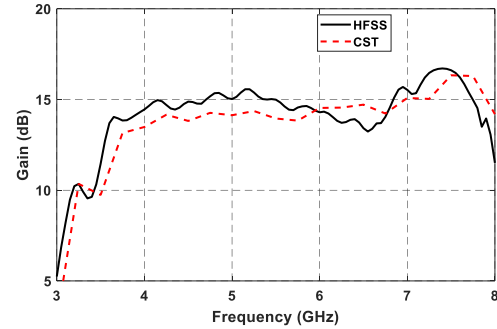


Fig. 18. The simulated peak gain for the sixteen-element linear array.

**Simulated radiation patterns**

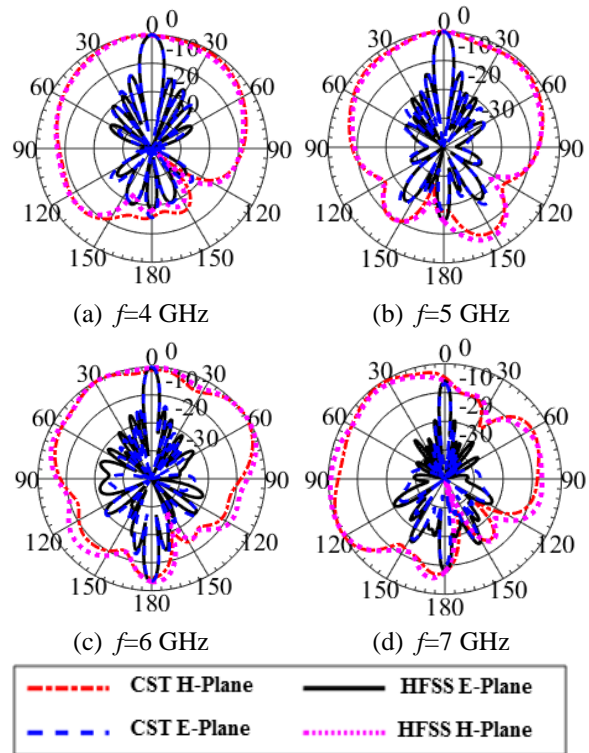


Fig. 19. The simulated normalized radiation patterns of the sixteen-element linear array at different frequencies.

The simulated radiation patterns for the sixteen-element RDRA linear array are plotted in Fig. 19. The co-polarized E-plane and H-plane are plotted using both HFSS and CST MWS. It could be seen that both software give almost the same results. The radiation patterns show a 10-dB front to back ratio through most of the band. The side lobe level (SLL) is between (-12 to -15) dB in the band. It could be seen from the radiation patterns that the beam width decreased as the frequency increased within the band at both the eight-element and sixteen-element array which is due to distance increase in wavelength [24]. The HPBW is varied between 10° at  $f=4$  GHz while

reached  $6^\circ$  at  $f=7$  GHz. The simulated cross polarization level was found less than -10 dB within the band according to both softwares. Table 6 shows the summary for the RDRA linear array designs for different elements number in this paper.

Table 6: Summary for the RDRA linear arrays

No. of Elements	Frequency Range (GHz)	BW %	Gain (dBi)	Antenna Size (mm)
1	4.3-7.4	53	5-6.5	40×50
2	3.9-7.9	67.8	8-10	60×60
4	3.57-7.85	75	10-12	70×100
8	3.7-8	73.5	12-14	90×200
16	3.57-7.95	76	14-17	110×390

Table 7 shows the HPBW value for both eight-element and sixteen-element RDRA linear array at different frequencies, while Table 8 shows some recent papers results obtained for the dielectric resonator antenna linear array with different element numbers.

Table 7: HPBW (E-plane) for the RDRA linear arrays

No. of Elements	$f=4$ GHz	$f=5$ GHz	$f=6$ GHz	$f=7$ GHz
2	$68.9^\circ$	$64.6^\circ$	$46.8^\circ$	$46.3^\circ$
4	$42.2^\circ$	$31.2^\circ$	$24.2^\circ$	$23.8^\circ$
8	$18.8^\circ$	$15.6^\circ$	$12.7^\circ$	$11.9^\circ$
16	$9.7^\circ$	$8^\circ$	$6.5^\circ$	$6^\circ$

Table 8: Recent papers results for linear array

No. of Elements	Ref #	Frequency Range (GHz)	Gain (dBi)	Antenna Size (mm)
2	5	3.85-6.2	4-6	$74 \times 52.7$
4	9	1.5-3.2	10-12	66.6 mm (between elements)
8	12	6.57-9.08	15.7	$250 \times 41.4$
15	7	8-12.5	10-12	23.5 mm (between elements)

## VIII. CONCLUSIONS

Rectangular dielectric resonator antenna (RDRA) linear arrays were designed, simulated and fabricated in this paper. The arrays with different element numbers, from two up to sixteen-element, were introduced. In order to isolate the spurious radiation from the feeder, the ground plane was placed on the top side of the substrate and directly underneath the RDRA. Multi section feeder was used to enhance the bandwidth which varies from 67% to 76%. A peak gain between 8 to 17 dBi were achieved for the different number of elements. Also, low side lobe level (SLL) were obtained in these designs, which was between (-10 to -18) dB for most of the arrays. Narrower beamwidth was obtained with  $6^\circ$  HPBW for

the sixteen-element linear array. Good agreement between HFSS and CST MWS simulated results and the measured results. The overall size for all designs is relatively small compare to other designs with the same element number.

## REFERENCES

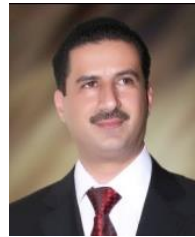
- [1] D. Soren, R. Ghatak, R. K. Mishra, and D. R. Poddar, "Dielectric resonator antennas designs and advances," *Electromagnetics Research*, vol. 60, pp. 195-213, 2014.
- [2] R. S. Yaduvanshi and H. Parthasarathy, *Rectangular Dielectric Resonator Antennas*. Springer India, 2016.
- [3] W. H. Kummer, "Basic array theory," *Proceeding of the IEEE*, vol. 80, no. 1, pp. 127-140, 1992.
- [4] C. A. Balanis, *Antenna Theory Analysis and Design*. John Wiley & Sons, 2005.
- [5] G. Das, A. Sharma, and R. K. Gangwar, "Two elements dual segment cylindrical dielectric resonator antenna array with annular shaped microstrip feed," *2016 Twenty Second National Conference on Communication (NCC)*, pp. 1-6, 2016.
- [6] A. Gupta and R. K. Gangwar, "Design, fabrication, and measurement of dual-segment rectangular dielectric resonator antenna array excited with conformal strip for S-band application," *Electromagnetics*, vol. 36, no. 4, pp. 236-248, 2016.
- [7] A. S. Al-Zoubi, A. A. Kishk, and A. W. Glisson, "A linear rectangular dielectric resonator antenna array fed by dielectric image guide with low cross polarization," *IEEE Transactions on Antenna and Propagation*, vol. 58, pp. 697-705, 2010.
- [8] A. S. Al-Zoubi, A. A. Kishk, and A. W. Glisson, "Aperture coupled rectangular dielectric resonator antenna array fed by dielectric image guide," *IEEE Transactions on Antennas and Propagation*, vol. 57, no. 8, pp. 2252-2259, 2009.
- [9] M. R. Nikkhah, A. A. Kishk, and J. Rashed-Mohassel, "Wideband DRA array placed on array of slot windows," *IEEE Transactions on Antenna and Propagation*, vol. 63, pp. 5382-5390, 2015.
- [10] M. Su, L. Yuan, and Y. Liu, "A linearly polarized radial line dielectric resonator antenna array," *IEEE Antennas and Wireless Propagation Letters*, vol. PP, no. 99, pp. 1-1, 2016.
- [11] W. M. Abdel-Wahab, D. Busuioc, and S. Safavi-Naeini, "Millimeter-wave high radiation efficiency planar waveguide series-fed dielectric resonator antenna (DRA) array: Analysis, design, and measurements," *IEEE Transactions on Antennas and Propagation*, vol. 59, no. 8, pp. 2834-2843, 2011.
- [12] J. Lin, W. Shen, and K. Yang, "A low sidelobe and wideband series fed linear dielectric resonator antenna array," *IEEE Antennas and Wireless Propagation Letters*, vol. PP, no. 99, pp. 1-1, Doi: 10.1109/LAWP.2016.2586579, 2016.
- [13] R. Khare and R. Nema, "Review of impedance

matching networks for bandwidth enhancement,” *International Journal of Emerging Technology and Advanced Engineering*, vol. 2, iss. 1, pp. 92-96, 2012.

- [14] R. K. Mongia, “Theoretical and experimental resonant frequencies of rectangular dielectric resonators,” *IEE Proc.-H*, vol. 139, pp. 98-104, 1992.
- [15] S. Fakhte and H. Oraizi, “Derivation of the resonant frequency of rectangular dielectric resonator antenna by the perturbation theory,” *ACES Journal*, vol. 31, no. 8, 2016.
- [16] A. S. Al-Zoubi, “Enhanced radiation patterns of a wide-band strip-fed dielectric resonator antenna,” *Jordanian Journal of Computers and Information Technology*, Dec. 2015.
- [17] A. Al-Zoubi and A. Kishk, “Wide band strip-fed rectangular dielectric resonator antenna,” *3rd European Conference on Antennas and Propagation*, Berlin, Germany, 23-27 Mar. 2009.
- [18] F. Abushakra and A. Al-Zoubi, “Wideband vertical T-shaped dielectric resonator antennas fed by coaxial probe,” *Jordan Journal of Electrical Engineering (JJEE)*, vol. 3, no. 4, pp. 250-258, 2017.
- [19] HFSS: High Frequency Structure Simulator Based on the Finite Element Method, version 11.1, ANSYS Corporation 2008.
- [20] CST STUDIO SUITE-3D EM Simulation Software by CST, version 11.0.
- [21] A. Vasylychenko, Y. Schols, W. Raedt, and G. Vandenbosch, “Quality assessment of computational techniques and software tools for planar antenna analysis,” *IEEE Antennas Propagations Magazine*, vol. 51, no. 1, pp. 23-38, 2009.
- [22] I. Gupta and A. Ksienski, “Effect of mutual coupling on the performance of adaptive arrays,” in *IEEE Transactions on Antennas and Propagation*, vol. 31, no. 5, pp. 785-791, 1983.
- [23] J. R. Baker-Jarvis, M. D. Janezic, B. F. Riddle, C. L. Holloway, N. G. Paulter, Jr., J. Blendell, *Dielectric and Conductor-Loss Characterization and Measurements on Electronic Packaging Materials*, National Institute of Standards and Technology, July 2001.
- [24] S. F. Maharimi, M. F. Abdul Malek, M. F. Jamlos, S. C. Neoh, and M. Jusoh, “Impact of spacing and number of elements on array factor,” *PIERS Proceedings*, Kuala Lumpur, Malaysia, 2012.



**Feras Z. Abushakra** received the B.Sc. degree in Communications and Electronics Engineering from the Jordan University of Science and Technology (JUST), Irbid, Jordan, in 2011. From 2014 to 2016, he joined the master program of the Communication Engineer Department at Al-Yarmouk University, Jordan, majoring in Wireless Communications. His researches focus on Ultra-wideband antennas and dielectric resonator antenna with different shapes and different feeding methods.



**Asem S. Al-Zoubi** received his B.Sc. degree of Electrical Engineering from Eastern Mediterranean University, Cyprus in 1993, the M.Sc. degree in Electrical Engineering from Jordan University of Science and Technology, Jordan in 1998, and the Ph.D. degree in Electrical Engineering from the University of Mississippi, USA, in 2008. Currently, he is an Associate Professor with the Department of Telecommunications Engineering in Yarmouk University, Jordan. His current research interests include dielectric resonator antennas and microstrip antennas. Al-Zoubi is a Member of the IEEE.



**Derar F. Hawatmeh** received the B.Sc. degree in Communications and Electronics Engineering from the Jordan University of Science and Technology (JUST), Jordan, in 2010. In 2010, he joined the master program of the Electrical Engineering Department in JUST. From 2012 to 2013, he was a Researcher with the R&D Department, Waseela-Integrated Telecommunication Solutions. He was an Instructor with the Network and Communications Engineering Department, Al Ain University of Science and Technology, Al Ain, UAE, from 2013 to 2014. In 2014, he joined the Center for Wireless and Microwave Information Systems, University of South Florida, Tampa, FL, USA, as a Graduate Research Assistant. His current research interests include the analysis and the design of planar antennas, 3-D antennas compact, planar, passive, and multi-frequency and ultra-wideband microwave components.